

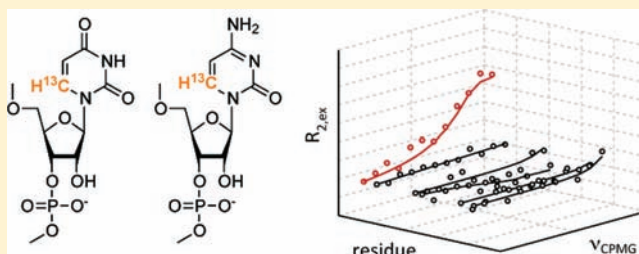
Synthesis of (6-¹³C)Pyrimidine Nucleotides as Spin-Labels for RNA Dynamics

Christoph H. Wunderlich, Romana Spitzer, Tobias Santner, Katja Fauster, Martin Tollinger, and Christoph Kreutz*

Institute of Organic Chemistry and Center for Molecular Biosciences Innsbruck (CMBI), University of Innsbruck, Innrain 80/82, 6020 Innsbruck, Austria

S Supporting Information

ABSTRACT: We present a ¹³C-based isotope labeling protocol for RNA. Using (6-¹³C)pyrimidine phosphoramidite building blocks, site-specific labels can be incorporated into a target RNA via chemical oligonucleotide solid-phase synthesis. This labeling scheme is particularly useful for studying milli- to microsecond dynamics via NMR spectroscopy, as an isolated spin system is a crucial prerequisite to apply Carr–Purcell–Meiboom–Gill (CPMG) relaxation dispersion type experiments. We demonstrate the applicability for the characterization and detection of functional dynamics on various time scales by incorporating the (6-¹³C)uridine and -cytidine labels into biologically relevant RNAs. The refolding kinetics of a bistable terminator antiterminator segment involved in the gene regulation process controlled by the preQ₁ riboswitch class I was investigated. Using ¹³C CPMG relaxation dispersion NMR spectroscopy, the milli- to microsecond dynamics of the HIV-1 transactivation response element RNA and the Varkud satellite stem loop V motif was addressed.



1. INTRODUCTION

Besides the structural characterization of biologically relevant macromolecules, solution NMR spectroscopy is perfectly suited to study dynamic features over a wide range of time scales, from nano- to milliseconds and beyond.^{1–4} Fast fluctuations in the nanosecond time regime can be characterized by the analysis of longitudinal and transverse relaxation rates and the hetero nuclear Overhauser effect (hetero-NOE) of ¹³C and ¹⁵N spins in the biomolecule of interest.^{4,5} Alternatively, residual dipolar couplings (RDCs) can be used to extract dynamic information on a biomolecule.^{4,6} The interpretation of the relaxation and RDC data to delineate quantitative information on the structural flexibility of a biomolecule can be a challenging task, e.g., if a motional coupling between local fluctuations and the overall tumbling rate of the molecule occurs.⁷ Order parameters ($0 < S^2 < 1$) are extracted via the model-free approach, giving information on the flexibility of a certain residue.^{8,9}

Motions in the micro- to millisecond time regime can be addressed using relaxation dispersion (RD) techniques.^{1,3,4} Structural adaptations of biomolecules in this time regime are often involved in functionally important processes, such as ligand binding or enzymatic reactions. Two experiments, the Carr–Purcell–Meiboom–Gill (CPMG) relaxation dispersion method and the determination of the power dependence of $R_{1\rho}$, are suitable to extract the exchange lifetimes between multiple states, the populations of the states, and the chemical shift difference between the states.¹ In proteins, both methods are routinely used to obtain information on backbone dynamics

by applying the techniques to the isolated amide ¹⁵N–¹H spin systems.¹⁰ In principle, nucleic acids would provide a similar spin system, namely, the NH protons of uridine (^{N³H}) and guanosine (^{N¹H}), which are involved in the formation of base pair hydrogen bonds. However, these protons often suffer from fast exchange with solvent protons, especially in single-stranded regions, where dynamic phenomena are commonly located. The broadening effect due to this chemical exchange can render the nitrogen-bound imino proton resonances unobservable. Alternatively, nonexchangeable ¹³C–¹H spin systems would provide information on the structural and dynamic changes occurring in single-stranded sequence regions of a nucleic acid.¹¹

A first mandatory step to study both structural and dynamic features of biomacromolecules is the introduction of an appropriate isotope labeling pattern.^{12–15} Currently, enzymatic methods to introduce uniformly ¹³C- and/or ¹⁵N-labeled nucleotides into RNA and DNA are state-of-the-art. Using these methods, nucleotide-specific labeling patterns (i.e., only adenosines/uridines or guanosines/cytidines) can be applied in a straightforward manner by mixing labeled and unlabeled (deoxy)ribonucleotide triphosphates in polymerase-catalyzed reactions.¹⁶ This labeling pattern, however, does impair to some extent the applicability of relaxation dispersion techniques.^{3,11} Very recently, to bypass problems caused by the uniform labeling pattern, site-specific ¹³C isotope labeling of RNA was

Received: March 4, 2012

Published: April 11, 2012

addressed.^{17–21} This is a crucial prerequisite to apply NMR methods for studying micro- to millisecond dynamics, as strong scalar coupling effects (e.g., ¹³C–¹³C couplings in ribose) or dipolar interactions with adjacent ¹³C or ¹⁵N spins are absent. These technical issues make relaxation dispersion experiments difficult to perform for nucleic acids as documented by the relatively small number of such studies so far.^{22–24} Besides enzymatic RNA/DNA synthesis, significant progress was made in the chemical synthesis of oligonucleotides. Commercially available DNA sequences comprising up to 100 nucleotides can be synthesized for biophysical investigations. RNA constructs, on the other hand, with up to 50 nucleotides can be produced in amounts suitable for NMR spectroscopic investigations. This approach offers the highest flexibility on placing isotope labeling and on the number of labels, but depends on the (labor-intensive) chemical synthesis of appropriate isotope ¹³C-modified phosphoramidites prior to sequence assembly.¹⁶ Our group recently introduced a near-native isotope labeling protocol relying on a 2'-O-¹³CH₃-modified uridine phosphoramidite precursor.²⁴ The 2'-O-¹³CH₃ spin-label was used to detect and quantify structural heterogeneity on a secondary structure level and further to probe milli- to microsecond dynamics by CPMG relaxation dispersion experiments. Within this work we present a fully native site-specific ¹³C labeling protocol for RNA. The proposed method uses (6-¹³C)-pyrimidine precursors to introduce isolated ¹³C–¹H spin systems into the target RNA via chemical synthesis.²⁵ The (6-¹³C)uridine and -cytidine residues proved to be appropriate labels to monitor functional micro- and millisecond dynamics of RNAs, as well as the kinetics of a secondary structure refolding reaction of a mRNA terminator antiterminator sequence involved in a gene regulation process.²⁶

2. EXPERIMENTAL SECTION

2.1. General Procedures. NMR spectra were acquired on a Varian 500 MHz Unity Plus instrument or a Bruker 300 MHz DRX instrument. Chemical shifts are reported relative to TMS and referenced to the residual proton solvent signal: CDCl₃ (7.26 ppm) for ¹H NMR spectra and CDCl₃ (77.0 ppm) for ¹³C spectra, DMSO-*d*₆ (2.50 ppm) for ¹H NMR spectra and DMSO-*d*₆ (39.52 ppm) for ¹³C spectra, and D₂O (4.79 ppm) for ¹H NMR spectra. ³¹P shifts are reported relative to external phosphoric acid (85%). ¹H assignments are based on gradient-selected correlation spectroscopy (COSY) experiments. ¹³C shifts are assigned from gradient-selected phase-sensitive heteronuclear single-quantum coherence (HSQC) and magnitude heteronuclear multiple-bond correlation (HMBC) experiments. Silica 60F-254 plates were used for TLC (thin-layer chromatography). For FC (flash column chromatography) silica gel 60 (230–400 mesh) was used. All reactions were conducted under an argon atmosphere. Reagents and solvents were purchased from Sigma-Aldrich and used without further purification. Organic solvents were extensively dried using freshly activated molecular sieves (4 Å).

2.2. Synthesis of the (6-¹³C)Uridine *tert*-Butyldimethylsilyl (TBDMS)- and [(Triisopropylsilyloxy)methyl (TOM)-Protected Phosphoramidites 8 and 10. **2.2.1. (3-¹³C)Cyanoacetic Acid (1).** 2-Bromoacetic acid (6.99 g, 50.3 mmol) was dissolved in 20 mL of water. Then sodium carbonate (Na₂CO₃; 3.4 g, 32.1 mmol) dissolved in 10 mL of water was added to reach pH 9. ¹³C-labeled potassium cyanide (3.24 g, 49 mmol) was dissolved in 10 mL of water and added to the deprotonated 2-bromoacetic acid. The reaction mixture was heated to 80 °C for 3 h and then stirred at room temperature for 20 h. The reaction was stopped by the addition of concentrated hydrochloric acid until pH 1. The solvent was evaporated and the residue dried in high vacuum for 30 min. Then (2-¹³C)cyanoacetic acid was extracted from the salt cake with 500 mL of diethyl ether. The ether was

evaporated, and the remaining yellow **1** was dried in high vacuum. Yield: 3.96 g (92%). ¹H NMR (300 MHz, DMSO-*d*₆, 25 °C): δ 3.46 (d, ²J_{CH} = 9.5 Hz, 2H, H₂C¹³C) ppm. ¹³C NMR (75 MHz, DMSO-*d*₆, 25 °C): δ 168.1 (COOH); 117.3 (CN); 26.0 (CH₂, d, ²J_{CC} = 59.4) ppm.

2.2.2. [(3-¹³C)Cyanoacetyl]urea (2). Compound **1** (2.0 g, 23.3 mmol) was treated with urea (1.5 g, 25 mmol) in 5 mL of acetic anhydride. The reaction mixture was heated to 90 °C for 30 min. After 5 min a white precipitate was formed. Then 8 mL of water was added, and stirring was continued for another 5 min. After the solution was cooled to room temperature, the precipitated **2** was filtered off and dried in high vacuum overnight. Yield: 2.68 g (90%). ¹H NMR (300 MHz, DMSO-*d*₆, 25 °C): δ 10.38 (s, 1H, NH); 7.35 (s, 2H, NH₂); 3.90 (d, ²J_{CH} = 10.0 Hz, 2H, H₂C¹³C) ppm. ¹³C NMR (75 MHz, DMSO-*d*₆, 25 °C): δ 168.08 (HNCOCH₂); 165.72 (H₂NCON); 115.6 (CN); 24.65 (CH₂, d, ¹J_{CC} = 61.5 Hz) ppm.

2.2.3. (6-¹³C)Uracil (3). Pd/BaSO₄ (5%, 800 mg) was suspended in 10 mL of 50% aqueous acetic acid in a 100 mL three-necked round-bottom flask. The palladium catalyst was treated several times with hydrogen by evacuating the flask followed by spilling it with hydrogen. Simultaneously, compound **2** (1.6 g, 12.5 mmol) was dissolved in 40 mL of boiling aqueous 50% acetic acid and then added to the reduced palladium catalyst. The reaction was stirred at room temperature under a hydrogen atmosphere for 36 h. Before being filtered through Celite, the mixture was heated to 70 °C for 1 h. The solvent was evaporated until a white precipitate was formed. Then **3** was precipitated by storing the suspension at 4 °C overnight. Compound **3** was filtered off and dried in high vacuum overnight. Yield: 1.15 g (82%). TLC (CH₂Cl₂/MeOH = 9/1): R_f = 0.3. ¹H NMR (300 MHz, DMSO-*d*₆, 25 °C): δ 10.64 (s, 2H, NH); 7.38 (dd, 1H, ¹J_{CH} = 180.6 Hz, ³J_{HH} = 7.5 Hz, C6H); 5.44 (dd, 1H, ²J_{CH} = 4.0 Hz, ³J_{HH} = 7.5 Hz, C5H) ppm. ¹³C NMR (75 MHz, DMSO-*d*₆, 25 °C): δ 164.31 (C4); 151.50 (C2); 142.17 (C6); 100.18 (d, ¹J_{CC} = 65.8 Hz, C5) ppm.

2.2.4. (2',3',5'-*O*-Tribenzoyl)(6-¹³C)Uridine (4). Compound **3** (560 mg, 5 mmol) was mixed with 1-*O*-acetyl-(2',3',5'-*O*-tribenzoyl)-β-D-ribofuranose (ATBR; 2.5 g, 5 mmol) and suspended in 20 mL of dry acetonitrile. Then bis(trimethylsilyl)acetamide (BSA; 3.7 mL, 15 mmol) was added, and the mixture was heated to 60 °C for 30 min, resulting in a clear solution. After the addition of trimethylsilyl trifluoromethanesulfonate ((TMS)OTf; 3.2 mL, 17.5 mmol), stirring at 60 °C was continued for another 30 min. The reaction was monitored by TLC, which showed complete conversion after the 1/2 h of stirring. The solvent was evaporated and the oily residue dried in high vacuum. The oil was dissolved in methylene chloride, and the organic phase was washed with saturated sodium bicarbonate solution, dried over sodium sulfate, and evaporated to give a yellow solid. Compound **4** was used without further purification in the next reaction. Yield: 2.73 g (98%). TLC (ethyl acetate/hexanes = 1/1): R_f = 0.8. ¹H NMR (300 MHz, CDCl₃, 25 °C): δ 8.66 (s, NH); 8.12–7.3 (m, 15H, CH(ar)); 7.4 (dd, 1H, ¹J_{CH} = 180.5 Hz, ³J_{HH} = 8.3 Hz, C6H); 6.31 (triplettoid, 1H, CH1'); 5.89 (dd, 1H, CH3'); 5.75 (dd, 1H, CH2'); 5.61 (dd, 1H, ²J_{CH} = 4.5 Hz, ³J_{HH} = 7.7 Hz, C5H); 4.84 (dd, 1H, CH5''); 4.70 (m, 1H, CH4'); 4.68 (dd, 1H, CH5') ppm. ¹³C NMR (75 MHz, CDCl₃, 25 °C): δ 139.69 (C6); 133.98, 133.83, 130.04, 129.80, 128.92, 128.70 (6 C(ar)); 104.66 (C5); 88.27 (C1'); 81.20 (C4'); 73.88 (C3'); 71.31 (C2'); 64.10 (C5') ppm.

2.2.5. (6-¹³C)Uridine (5). Crude compound **4** (2.5 g, 4.5 mmol) was treated with 15 mL of methylamine in ethanol (8 M) for 16 h under an argon atmosphere. After evaporation of the solvent, the oily residue was dissolved in water and the *N*-methylbenzamide was removed by extensive washing of the aqueous phase with methylene chloride. The aqueous phase was evaporated to dryness, and the resulting yellow foam was recrystallized from ethanol to give **5**. Yield: 1.1 g (90% referring to (6-¹³C)uracil). TLC (CH₂Cl₂/MeOH = 9/1): R_f = 0.1. ¹H NMR (300 MHz, D₂O, 25 °C): δ 7.75 (dd, 1H, ¹J_{CH} = 184.14 Hz, ³J_{HH} = 8.0 Hz, C6H); 5.79 (m, 1H, CH1'); 5.77 (m, C5H); 4.11 (triplettoid, 1H, CH2'); 4.23 (triplettoid, 1H, CH3'); 4.01 (dd, 1H, CH4'); 3.80 (dd, 1H, CH5''); 3.68 (dd, 1H, CH5') ppm. ¹³C NMR (75 MHz, D₂O, 25 °C): δ 165.6 (C4); 141.38 (C6); 151.27 (C2); 101.79 (d, ¹J_{CC} = 67.2

Hz, C5); 88.92 (C1'); 83.74 (C4'); 73.19 (C2'); 68.96 (C3'); 60.28 (C5') ppm.

2.2.6. 5'-O-(4,4'-Dimethoxytrityl)(6-¹³C)uridine (6). **5** (1.0 g, 4.1 mmol) was coevaporated three times with anhydrous pyridine and then dissolved in 5 mL of anhydrous pyridine. Then (4,4'-dimethoxytriphenyl)methyl chloride ((DMT)Cl; 1.7 g, 5.0 mmol) was added in three portions within 1 h. The reaction mixture was stirred for 4 h at room temperature. TLC showed nearly complete conversion at that time point. The solvent was evaporated and the residue coevaporated three times with toluene. The orange foam was dried in high vacuum and then dissolved in methylene chloride. The organic phase was washed with 5% citric acid, water, and saturated sodium bicarbonate solution, dried over sodium sulfate, and evaporated to dryness. The crude product was further purified by column chromatography (CC) on silica (CH₂Cl₂/methanol = 99/1 → 95/5 + 1% NEt₃) to give compound **6**. Yield: 1.5 g (67%). TLC (CH₂Cl₂/MeOH = 9/1): *R*_f = 0.4. ¹H NMR (300 MHz, CDCl₃, 25 °C): δ 10.35 (s, NH); 8.02 (dd, 1H ¹J_{CH} = 183.94 Hz, ³J_{HH} = 8.0 Hz, C6H); 7.40–7.18 (m, 9 CH(ar)); 6.88–6.77 (m, 4 CH(ar)); 5.90 (triplettoid, 1H, CHI'); 5.49 (s, C2'OH); 5.35 (triplettoid, 1H, CSH); 4.43 (triplettoid, 1H, CH3'); 4.35 (triplettoid, 1H, CH2'); 4.17 (dd, 1H, CH4'); 3.54 (dd, 1H, CH5''); 3.77 (s, 6H, 2 OCH₃); 3.48 (dd, 1H, CH5'); 3.40 (duplettoid, 1H, C3'OH) ppm. ¹³C NMR (75 MHz, CDCl₃, 25 °C): δ 167.50 (C4); 158.82 (C(ar)); 151.30 (C2); 140.62 (C6); 135.45 (C(ar)); 130.28, 128.15, 113.44 (C(ar)); 106.82 (C5); 90.14 (C1'); 87.16 (C4'); 75.70 (C2'); 69.40 (C3'); 62.10 (C5'); 55.37 (OCH₃) ppm. ESI-MS (*m/z*): [M + H]⁺ calcd for (¹³C)₂₉H₃₀N₂O₈, 547.56; found, 547.29.

2.2.7. 5'-O-(4,4'-Dimethoxytrityl)-2'-O-(tert-butyl dimethylsilyl)(6-¹³C)uridine (7). Compound **6** (1.5 g, 2.74 mmol) was dissolved in anhydrous tetrahydrofuran (THF; 12 mL). Silver nitrate (AgNO₃; 695 mg, 4.11 mmol) and pyridine (664 μL, 8.22 mmol) were added, and the suspension was stirred for 1/2 h in the dark. Then tert-butyl dimethylsilyl chloride ((TBDMS)Cl; 620 mg, 4.11 mmol) was added, and the mixture was stirred for 4 h at room temperature in the dark. The suspension was filtered over Celite, and the filtrate was evaporated to dryness. The residue was dried in high vacuum and then dissolved in methylene chloride. The organic phase was washed with saturated sodium bicarbonate solution, dried over sodium sulfate, and evaporated to dryness. The crude product was further purified by CC on silica (CH₂Cl₂/ethyl acetate = 100/0 → 80/20) to give compound **7**. Yield: 1.0 g (55%). TLC (CH₂Cl₂/ethyl acetate = 6/4): *R*_f = 0.71. ¹H NMR (300 MHz, DMSO-*d*₆, 25 °C): δ 8.56 (s, NH); 7.75 (dd, 1H, ¹J_{CH} = 181.33 Hz, ³J_{HH} = 7.8 Hz, C6H); 5.30 (triplettoid, 1H, CSH); 7.41–7.15 (m, 9 CH(ar)), 6.95–6.86 (m, 4 CH(ar)); 5.76 (triplettoid, 1H, CHI'); 5.11 (duplettoid, 1H, C3'OH); 4.21 (triplettoid, 1H, CH2'); 4.05 (triplettoid, 1H, CH3'); 4.00 (m, 1H, CH4'); 3.4–3.2 (m, 2H, CH5'' and CH5'); 3.74 (s, 6H, 2 OCH₃); 0.86 (s, 9H, SiC(CH₃)₃); 0.06 (s, 6H, Si(CH₃)₂) ppm. ¹³C NMR (75 MHz, DMSO-*d*₆, 25 °C): δ 162.92 (C4); 158.82 (C(ar)); 150.46 (C2); 144.65 (C(ar)); 150.05 (C6); 135.20, 127.70, 126.81, 113.26 (C(ar)); 101.43 (d, ¹J_{CC} = 67.4 Hz, C5); 88.53 (C1'); 85.93 (C4'); 75.52 (C2'); 69.36 (C3'); 62.71 (C5') 55.05 (OCH₃); 25.62 (SiC(CH₃)₃); 17.82 (SiC(CH₃)₂); –5.07 (Si(CH₃)₂) ppm. ESI-MS (*m/z*): [M + H]⁺ calcd for (¹³C)₃₅H₄₄N₂O₈Si, 661.82; found, 661.42.

2.2.8. 5'-O-(4,4'-Dimethoxytrityl)-2'-O-(tert-butyl dimethylsilyl)(6-¹³C)uridine 3'-O-(2'-Cyanoethyl N,N-diisopropylphosphoramidite) (8). Anhydrous tetrahydrofuran (4 mL) and N,N-diisopropylethylamine (DIPEA; 523 μL, 3.0 mmol) were mixed. Then compound **7** (400 mg, 0.6 mmol) was added, and the clear solution was stirred for 15 min. Then 2'-cyanoethyl N,N-diisopropylchlorophosphoramidite ((CEP)Cl; 343 mg, 1.2 mmol) was added dropwise. The reaction was monitored by TLC. After 2 h the reaction mixture was diluted with methylene chloride and washed with half-saturated sodium bicarbonate solution. The organic phase was dried over sodium sulfate and evaporated to dryness. The crude product was further purified by CC on silica (ethyl acetate/hexanes = 50/50 + 1% NEt₃) to give compound **8** as a mixture of diastereoisomers. Yield: 422 mg (83%). TLC (ethyl acetate/hexanes = 1/1): *R*_f = 0.48. ¹H NMR (300 MHz, CDCl₃, 25 °C): δ 7.99 (dd, 1H ¹J_{CH} = 181.73 Hz, ³J_{HH} = 8.13 Hz,

C6H); 7.45–7.15 (m, 9 CH(ar)); 6.90–6.77 (m, 4 CH(ar)); 5.99 (triplettoid, 1H, CHI'); 5.31 (m, 1H, CSH); 4.44 (triplettoid, 1H, CH2'); 4.33 (m, 1H, CH3'); 4.22 (m, 1H, CH4'); 4.12 (ddd, 1H, ²J_{HH} = 7.2 Hz, –CH₂OP); 3.80 (s, 6H, 2 OCH₃); 3.75–3.60 (m, 1H, ²J_{HH} = 7.2 Hz, –CH₂OP); 3.58 (m, 2H, 2 CH(iPr)); 3.45–3.35 (m, 2H, CH5'' and CH5'); 2.64 (t, 1H, ²J_{HH} = 6.4 Hz, –CH₂CN); 2.40 (t, 1H, ²J_{HH} = 6.4 Hz, –CH₂CN); 1.33–1.12 (duplettoid, 9H, ³J_{HH} = 6.7 Hz, 3 CH₃(iPr)); 1.11–0.98 (d, 3H, ³J_{HH} = 6.7 Hz, CH(iPr)); 0.95–0.77 (s, 9H, SiC(CH₃)₃); 0.02–0.2 (m, 6H, Si(CH₃)₂) ppm. ¹³C NMR (75 MHz, CDCl₃, 25 °C): δ 140.43 (C6) ppm. ³¹P NMR (121 MHz, CDCl₃, 25 °C): δ 150.27, 150.74 ppm. ESI-MS (*m/z*): [M + H]⁺ calcd for (¹³C)₄₄H₆₁N₄O₉PSi, 862.04; found, 862.40.

2.2.9. 5'-O-(4,4'-Dimethoxytrityl)-2'-O-[[Triisopropylsilyl]oxy]methyl(6-¹³C)uridine (9). **6** (616 mg, 1.13 mmol) was dissolved with DIPEA (765 μL, 4.5 mmol) in 10 mL of 1,2-dichloroethane (DCE). To the clear solution was added dibutyltin dichloride (Bu₂SnCl₂; 616 mg, 2.02 mmol), and the reaction mixture was stirred for 1 h at room temperature. After the mixture was heated to 80 °C, [(triisopropylsilyl)oxy]methyl chloride ((TOM)Cl; 276 mg, 1.24 mmol) was added. After 30 min the reaction mixture was cooled to room temperature and diluted with methylene chloride. The organic phase was then washed with saturated sodium bicarbonate solution and water, dried over sodium sulfate, and filtered over Celite. The organic phase was then evaporated to dryness. The residual yellow foam was further purified by CC on silica (ethyl acetate/hexanes = 20/80 → 60/40) to give compound **9**. Yield: 240 mg (30%). TLC (ethyl acetate/hexanes = 5/5): *R*_f = 0.6. ¹H NMR (300 MHz, CDCl₃, 25 °C): δ 7.93 (dd, 1H ¹J_{CH} = 182.44 Hz, ³J_{HH} = 8.2 Hz, C6H); 7.41–7.13, 6.89 (m, 13 CH(ar)); 6.02 (triplettoid, 1H, CHI'); 5.28 (m, 1H, CSH); 5.05 (d, 1H, C3'OH); 5.02–4.97 (dd, 2H, ²J_{HH} = 4.99 Hz, –OCH₂OSi); 4.26 (triplettoid, 1H, CH2'); 4.16 (dd, 1H, CH3'); 3.95 (dd, 1H, CH4'); 3.74 (s, 6H, 2 –OCH₃); 3.25 (dd, 1H, CH5''); 3.20 (dd, 1H, CH5'); 1.20–1.17 (m, 3H, SiCH(CH₃)₂); 1.01–0.95 (m, 18H, SiCH(CH₃)₂) ppm. ¹³C NMR (75 MHz, CDCl₃, 25 °C): δ 162.28 (C4); 158.30 (C(ar)); 149.56 (C2); 143.90 (C(ar)); 139.73 (C6); 134.7 (C(ar)); 129.71 (C(ar)); 127.59 (C(ar)); 126.75 (C(ar)); 112.89 (C(ar)); 102.20 (C5); 101.31 (C1'); 90.24 (CAr3); 87.41 (O2'CH₂O); 86.73 (C4'); 83.28 (C2'); 69.00 (C3'); 61.73 (C5'); 54.84 (2 –OCH₃); 17.38 (SiCH(CH₃)₂); 11.45 (SiCH(CH₃)₂) ppm.

We also isolated the 3'-regioisomer 5'-O-DMT-3'-O-TOM-(6-¹³C)-uridine for repeated tomylation reactions. Yield: 231 mg (28%). TLC (ethyl acetate/hexanes = 5/5): *R*_f = 0.4. ¹H NMR (300 MHz, CDCl₃, 25 °C): δ 8.13 (s, 1H, NH); 7.76 (dd, 1H, ¹J_{CH} = 181.34 Hz, ³J_{HH} = 8.11 Hz, C6H); 7.41–7.18 (m, 9H, CH(ar)); 6.87–6.77 (m, 4H, CH(ar)); 5.95 (triplettoid, 1H, CHI'); 5.39 (m, 1H, CSH); 5.07–4.89 (dd, 2H, ²J_{HH} = 4.91 Hz, –OCH₂OSi); 4.32 (m, 1H, CH3'); 4.27 (m, 1H, CH2'); 3.79 (s, 6H, –OCH₃); 3.56 (dd, 1H, CH5''); 3.41 (dd, 1H, CH5'); 3.36 (dd, 1H, CH4'); 1.25 (t, 3H, SiCH(CH₃)₂); 1.06 (m, 18H, SiCH(CH₃)₂) ppm.

The 3'-regioisomer 5'-O-DMT-3'-O-TOM-(6-¹³C)uridine was isolated and treated with 2 mL of 1 M tetrabutylammonium fluoride (TBAF) in acetonitrile. After 3 h TLC indicated complete removal of the silyl protection group. The solvent was evaporated and the residual oil dried in high vacuum. The oil was dissolved in methylene chloride and the organic phase washed with saturated sodium bicarbonate solution and water, dried over sodium sulfate, and evaporated to dryness. Crude compound **6** was purified by column chromatography on silica (CH₂Cl₂/methanol = 99/1 → 95/5 + 1% NEt₃, analytical data identical to those of compound **6**) and was again used for the tomylation reaction.

2.2.10. 5'-O-(4,4'-Dimethoxytrityl)-2'-O-[[Triisopropylsilyl]oxy]methyl(6-¹³C)uridine 3'-O-(2'-Cyanoethyl N,N-diisopropylphosphoramidite) (10). Anhydrous methylene chloride (5 mL) and N,N-dimethylethylamine (DMEA; 540 μL, 5.0 mmol) were mixed. Then compound **9** (720 mg, 0.98 mmol) was added, and the clear solution was stirred for 15 min. Then (CEP)Cl (350 mg, 1.5 mmol) was added dropwise. The reaction was monitored by TLC. After 2 h the reaction mixture was diluted with methylene chloride and washed with half-saturated sodium bicarbonate solution. The organic phase was dried over sodium sulfate and evaporated to dryness. The crude product was

further purified by CC on silica (ethyl acetate/hexanes = 50/50 → 60/40 + 1% NEt₃) to give compound **10** as a mixture of diastereoisomers. Yield: 784 mg (86%). TLC (ethyl acetate/hexanes = 1/1): R_f = 0.55. ¹H NMR (500 MHz, CDCl₃, 25 °C): δ 8.02 (s, 1H, NH); 7.86 (dd, 1H, ¹J_{CH} = 181.46 Hz, ³J_{HH} = 8.25 Hz, C6H); 5.36 (dd, 1H, C5H); 7.47–7.21, 6.86–6.80 (m, 13 CH(ar)); 6.12 (m, 1H, CH1'); 5.35 (m, 2H, ²J_{HH} = 4.84 Hz, –OCH₂OSi); 4.41 (m, 1H, CH2'); 4.46 (m, 1H, CH3'); 4.27 (m, 1H, CH4'); 3.60 (dd, 1H, CH5''); 3.98–3.84 (m, 1H, POCH₂); 3.71–3.35 (m, 3 × 1H, POCH₂, CHS', NCH(CH₃)₂); 3.79 (s, 6H, –OCH₃); 2.64 (m, 1H, –CH₂CN); 2.39 (m, 1H, ²J_{HH} = 6.35 Hz, –CH₂CN); 1.58 (s, 3H, –SiCH(CH₃)₂); 1.23–1.10 (m, 12H, –NCH(CH₃)₂); 1.10–0.99 (m, 18H, SiCH(CH₃)₂) ppm. ³¹P NMR (201 MHz, CDCl₃, 25 °C): δ 150.53, 150.11 ppm. ESI-MS (m/z): [M + H]⁺ calcd for (¹³C₁)C₄₈H₆₉N₄O₁₀PSi, 934.14; found, 934.37.

2.3. Synthesis of the (6-¹³C)Cytidine TOM-Protected Phosphoramidite **14.** **2.3.1. 3'-O-Acetyl-5'-O-(4,4'-dimethoxytrityl)-2'-O-[[[(triisopropylsilyloxy)methyl]](6-¹³C)uridine (**11**).** Compound **9** (350 mg, 0.47 mmol) was dissolved in 700 μL of anhydrous pyridine. Then 4-(dimethylamino)pyridine (DMAP; 5.7 mg, 0.05 mmol) was added. After the mixture was cooled to 0 °C, acetic anhydride (Ac₂O; 48 μL, 0.51 mmol) was added. The ice bath was removed, and the reaction mixture was stirred for 2 h at room temperature. The solvent was evaporated and the residue twice coevaporated with toluene. The residue was then dissolved in methylene chloride and washed with 5% citric acid, water, and saturated sodium bicarbonate solution. The organic phase was dried over sodium sulfate and then evaporated. The foam was dried in high vacuum and then purified by CC on silica (ethyl acetate/hexanes = 50/50) to give compound **11**. Yield: 300 mg (82%). TLC (ethyl acetate/hexanes = 1/1): R_f = 0.7.

Compound **11** was used without further characterization in the next steps.

2.3.2. 5'-O-(4,4'-Dimethoxytrityl)-2'-O-[[[(triisopropylsilyloxy)methyl]](6-¹³C)cytidine (12**).** Step a: Anhydrous methylene chloride (4 mL) was mixed with triethylamine (Et₃N; 528 μL, 3.8 mmol). Then compound **11** (300 mg, 0.38 mmol) and DMAP (6.0 mg, 0.05 mmol) were added. After 10 min, 2,4,6-trisopropylbenzenesulfonyl chloride ((TPS)Cl; 176 mg, 0.58 mmol) was added in small portions, and the reaction was stirred for 4 h at room temperature. Then the reaction mixture was diluted with methylene chloride, and the organic phase was washed with half-saturated sodium bicarbonate solution, dried over sodium sulfate, and evaporated to dryness. The resulting foam was dried in high vacuum.

Step b: The crude product of the previous step was dissolved in 4 mL of tetrahydrofuran and then treated with 4 mL of 28% aqueous ammonia. The mixture was stirred for 18 h at room temperature.

Step c: After 18 h, 4 mL of methylamine solution in ethanol (8 M) was added to the yellow suspension, resulting in a clear solution. The reaction was continued for 45 min until TLC showed the removal of the 3'-O-acetyl protection group. The solvent was then evaporated and the residual oil dried in high vacuum. The oil was dissolved in methylene chloride, washed with saturated sodium bicarbonate solution, and dried over sodium sulfate and the solvent evaporated. The resulting foam was purified by column chromatography on silica (CH₂Cl₂/methanol = 99/1 → 95/5) to yield compound **12**. Yield: 190 mg (68% referred to compound **11**). TLC (CH₂Cl₂/methanol = 96/4): R_f = 0.45. ¹H NMR (300 MHz, DMSO-*d*₆, 25 °C): δ 7.68 (dd, 1H ¹J_{CH} = 178.59 Hz, ³J_{HH} = 7.30 Hz, C6H); 7.41–7.20 (m, 13 CH(ar)); 5.94 (triplettoid, 1H, CH1'); 5.54 (dd, 1H, C5H); 5.12 (dd, 2H, ²J_{HH} = 4.7 Hz, –OCH₂OSi); 4.30 (dd, 1H, CH3'); 4.18 (m, 1H, CH2'); 4.10 (dd, 1H, CH4'); 3.79 (s, 6H, –OCH₃); 3.51 (m, 2 × 1H, CHS' and CHS''); 3.15 (d, 1H, C3'OH); 1.57 (s, 3H, SiCH(CH₃)₂); 1.30–1.10 (m, 18H, SiCH(CH₃)₂) ppm. ¹³C NMR (75 MHz, DMSO-*d*₆, 25 °C): δ 164.43 (C4); 158.30 (C(ar)); 151.73 (C2); 144.95 (C(ar)); 143.83 (C6); 132.64 (C(ar)); 130.05 (C(ar)); 127.5 (C(ar)); 116.13 (C(ar)); 98.65 (C5); 94.8 (C(quart)); 90.40 (C1'); 87.41 (O2'CH₂O); 71.66 (C4'); 80.90 (C2'); 71.66 (C3'); 63.68 (C5'); 57.75 (–OCH₃); 19.94 (CHSi); 14.45 (CH₃CHSi) ppm.

2.3.3. N⁴-Acetyl-5'-O-(4,4'-dimethoxytrityl)-2'-O-[[[(triisopropylsilyloxy)methyl]](6-¹³C)cytidine (13**).** Compound **12** (190 mg, 0.26 mmol) was dissolved in 1 mL of anhydrous dimethylformamide (DMF) followed by the addition of Ac₂O (25 μL, 0.26 mmol). The reaction was stirred for 22 h at room temperature. Then a few drops of methanol were added. The solvent was evaporated and the oily residue dissolved in methylene chloride. The organic phase was washed with saturated sodium bicarbonate solution, dried over sodium sulfate, and evaporated to dryness. The crude product was further purified by CC on silica (CH₂Cl₂/methanol = 99/1 → 98/2) to give compound **13**. Yield: 180 mg (89%). TLC (ethyl acetate/hexanes = 7/3): R_f = 0.38. ¹H NMR (300 MHz, CDCl₃, 25 °C): δ 8.58 (s, NH); 8.48 (dd, 1H, ¹J_{CH} = 183.67 Hz, ³J_{HH} = 7.33 Hz, C6H); 7.47–7.20 (m, 13 CH(ar)); 7.04 (dd, 1H, C5H); 6.02 (triplettoid, 1H, CH1'); 5.21 (dd, 2H, ¹J_{HH} = 4.7 Hz, –OCH₂OSi); 4.22 (m, 1H, CH2'); 4.37 (m, 1H, CH3'); 4.09 (dd, 1H, CH4'); 3.81 (s, 6H, 2 –OCH₃); 3.60 (dd, 1H, CH5''); 3.52 (dd, 1H, CH5'); 3.33 (d, 1H, C3'OH); 2.21 (s, 3H, –CONHCH₃); 1.61 (s, 3H, CH(iPr)); 1.30–0.98 (m, 18H, 3 CH₃(iPr)) ppm. ¹³C NMR (75 MHz, CDCl₃, 25 °C): δ 169.77 (HNCOCH₃); 162.68 (C4); 158.83 (C(ar)); 155.09 (C2); 145.05 (C6); 140.27 (C(ar)); 138.28 (C(ar)); 130.31 (C(ar)); 128.31 (C(ar)); 127.25 (C(ar)); 113.44 (C(ar)); 98.65 (C5); 90.25 (C1'); 90.29 (O2'CH₂O); 87.31 (C(quart)); 83.51 (C4'); 83.29 (C2'); 68.21 (C3'); 61.30 (C5'); 55.38 (–OCH₃); 25.11 (NHCOCH₃); 17.91 (CH₃CHSi); 11.99 (CH₃CHSi) ppm.

2.3.4. N⁴-Acetyl-5'-O-(4,4'-dimethoxytrityl)-2'-O-[[[(triisopropylsilyloxy)methyl]](6-¹³C)cytidine 3'-(2'-Cyanoethyl N,N-diisopropylphosphoramidite) (14**).** Anhydrous methylene chloride (5 mL) and DMEA (250 μL, 2.3 mmol) were mixed. Then compound **13** (130 mg, 0.23 mmol) was added, and the clear solution was stirred for 15 min. Then (CEP)Cl (83 mg, 0.35 mmol) was added dropwise. The reaction progress was monitored by TLC. After 2 h the reaction mixture was diluted with methylene chloride and washed with half-saturated sodium bicarbonate solution. The organic phase was dried over sodium sulfate and evaporated to dryness. The crude product was further purified by CC on silica (ethyl acetate/hexanes = 70/30 + 1% NEt₃) to give compound **14** as a mixture of diastereoisomers. Yield: 205 mg (91%). TLC (ethyl acetate/hexanes = 7/3): R_f = 0.46. ¹H NMR (300 MHz, CDCl₃, 25 °C): δ 8.59 (s, 1H, NH); 8.47 (dd, 1H, ¹J_{CH} = 182.48 Hz, ³J_{HH} = 7.41 Hz, C6H); 7.47–7.19 (m, 13 CH(ar)); 6.98 (dd, 1H, C5H); 6.15 (triplettoid, 1H, CH1'); 5.20 (m, 2H, ¹J_{HH} = 4.7 Hz, –OCH₂OSi); 4.51 (m, 1H, CH3'); 4.36 (m, 1H, CH2'); 4.33 (m, 1H, CH4'); 3.98–3.84 (m, 1H, POCH₂); 3.81 (s, 6H, 2 –OCH₃); 3.69 (dd, 1H, CH5''); 3.73–3.40 (m, 1H, POCH₂, CHS', NCHMe₂); 2.60 (m, 1H, –CH₂CN); 2.40 (t, 1H, ²J_{HH} = 6.4 Hz, –CH₂CN); 2.19 (s, 3H, CONHCH₃); 1.61 (s, 3H, CH(iPr)(TOM)); 1.17 (m, 1H, NCHMe₂(CEP)); 1.21–1.10 (m, 12H, NCH(CH₃)₂); 1.10–0.93 (m, 18H, SiCH(CH₃)₂(TOM)) ppm. ³¹P NMR (121 MHz, CDCl₃, 25 °C): δ 150.84, 150.58 ppm. ESI-MS (m/z): [M + H]⁺ calcd for (¹³C₁)C₅₀H₇₂N₅O₁₀PSi, 975.20; found, 975.41.

2.4. Chemical Synthesis of RNA Oligonucleotides on a Solid Support. The ¹³C-modified phosphoramidites were used in combination with standard 2'-O-TOM-protected building blocks (ChemGenes) to synthesize RNA sequences **15**, **16**, **17**, and **18**. Custom primer support PS 200 (GE Healthcare) with an average loading of 80 μmol g^{−1} was used. The sequences were synthesized on an Applied Biosystems 391 PCR Mate using self-written RNA synthesis cycles. Amidite (0.1 M) and activator (5-(benzylthio)-1H-tetrazole, 0.25 M) solutions were dried over freshly activated molecular sieves overnight.

The removal of protecting groups and the cleavage from the solid support were achieved by treatment with aqueous methylamine (40%, 650 μL) and ethanolic methylamine (8 M, 650 μL) at room temperature for 6–8 h. After evaporation of the alkaline deprotection solution, the 2'-O-protecting groups were removed by adding 1 M TBAF in THF (1200 μL). After 16 h at 37 °C, the reaction was quenched by the addition of 1 M triethylammonium acetate (TEAA; pH 7.0, 1200 μL). The volume was reduced to approximately 1 mL, and then the solution was applied to a HiPrep 26/10 desalting column

(GE Healthcare). The crude RNAs were eluted with water, evaporated to dryness, and dissolved in 1 mL of water.

The quality of the crude RNAs was checked via anion exchange chromatography on a Dionex DNAPac PA-100 column (4 × 250 mm) using our standard eluents and at elevated temperature (80 °C).²⁴ Purification of the RNA sequences was achieved by applying the crude RNA on a semipreparative Dionex DNAPac PA-100 column (9 × 250 mm). The fractions containing the desired RNA were pooled and loaded onto a C18 SepPak cartridge (Waters) to remove HPLC buffer salts. The RNA triethylammonium salt form was then eluted from the C18 column with water/acetonitrile (1/1, v/v) and lyophilized. To obtain the RNA sodium salt form, the RNAs were treated with a sodium chloride solution (250 mM, 2 × 10 mL) and water (3 × 10 mL) in a Vivaspin 20 ultracentrifugation unit with a molecular weight cutoff of 3000 (Satorius Stedim). The integrity of the RNAs was further checked by mass spectrometry on a Finnigan LCQ Advantage MAX ion trap instrument connected to an Amersham Ettan micro-LC instrument (GE Healthcare).

2.5. NMR Spectroscopy. RNA samples were lyophilized as the sodium salts and dissolved in the appropriate buffer in 9/1 H₂O/D₂O or pure D₂O. The HIV-1 transactivation response element (TAR) RNAs **15** and **16** were dissolved in 15 mM sodium phosphate buffer (pH 6.4) and 25 mM sodium chloride. The 6-¹³C-¹H pyrimidine resonance assignments for this RNA are reported in the literature.⁷ The Varkud satellite stem loop V motif **17** was dissolved in 10 mM Tris-HCl buffer (pH 6.5) and 25 mM NaCl. The 6-¹³C-¹H pyrimidine resonances of this RNA were previously assigned.²⁷ The bistable RNA **18** involved in the gene regulation process by the preQ₁ riboswitch was dissolved in 25 mM sodium arsenate buffer, pH 6.5.

NMR experiments on 6-¹³C-modified RNA sequences were conducted either on a Bruker 600 MHz Avance II+ instrument or on Varian Unity instruments operating at 800 or 500 MHz proton Larmor frequency. The ¹H 1D NMR spectra of H₂O samples were acquired using a double-pulsed field gradient spin-echo pulse sequence.²⁸ The 2D ¹H-¹³C correlation spectra were acquired via double INEPT (insensitive nuclei enhanced by polarization transfer) using sensitivity improvement in phase-sensitive mode, echo/antiecho TPPI (time proportional phase incrementation) gradient selection with decoupling during acquisition, trim pulses in INEPT transfer, and shaped pulses for all 180° pulses on the carbon channel and with gradients in back-INEPT (Bruker pulse program hsqcetgpsisp2.2). The 2D heteronuclear correlation spectra were processed using nmrPipe and visualized using nmrDraw.²⁹

¹³C CPMG relaxation dispersion experiments on RNA sequences **15**, **16**, and **17** were recorded at 11.7 and 18.8 T using the pulse sequence previously published with CPMG field strengths of 80, 80, 160, 240, 320, 400, 480, 560, 640, 640, 720, 800, 880, and 960 Hz.³⁰ The relaxation delay τ_{CP} was set to 25 ms. A total of 1024 × 64 (1024 × 64) complex data points were recorded at 18.8 (11.7) T with the spectral widths in the proton and carbon dimensions set to 12775 and 3000 Hz (8000 and 1875 Hz), respectively. The number of transients was set to 40 at 18.8 and 11.7 T, and the interscan delay was set to 1.3 or 1.8 s, yielding total experimental times of 32 or 44 h.

Longitudinal exchange (ZZ) and longitudinal relaxation (T_1) experiments are based on pulse sequences recently published.³¹ For a 1 mM sample of sequence **18**, arrays of T_1 and ZZ exchange spectra were recorded at 11.7 T at 306 K with mixing periods of 10, 50, 100, 200, 300, 400, 600, and 800 ms. The size of the data matrices for each spectrum was 5000 × 1500 complex data points, the number of scans was 64, and the interscan delay was 1.2 s to yield a total measuring time of 22 h.

2.6. NMR Data Analysis. Spectral processing and peak picking and integration were performed using nmrPipe and the nmrDraw software package.²⁹ All subsequent steps were performed using in-house-written software written in Matlab (The MathWorks, www.mathworks.com).

2.6.1. Processing and Analysis of CPMG RD Data. Peak intensities at the various CPMG fields were obtained by summing over 3 × 3 or 1 × 1 ($t_1 \times t_2$) data points using the serT script implemented in the

nmrPipe package. These intensities were used to calculate effective transverse relaxation rates $R_{2,eff}$ according to

$$R_{2,eff} = -\frac{1}{\tau_{CP}} \ln \frac{I(\nu_{CPMG})}{I_0} \quad (1)$$

with τ_{CP} the relaxation delay, $I(\nu_{CPMG})$ the peak intensity at the CPMG frequency ν_{CPMG} , and I_0 the peak intensity from the reference experiment. The transverse relaxation rates were used as the experimental input for fitting the dispersion profiles. The data were fit according to a general expression for the intermediate exchange regime (Carver–Richards equation³²):

$$R_{2,eff} = R_{2,0} + \frac{k_{ex}}{2} - \nu_{CPMG} \cosh^{-1}[D_+ \cosh(\eta_+) - D_- \cosh(\eta_-)] \quad (2)$$

with

$$D_{\pm} = \frac{1}{2} \left[\pm 1 + \frac{\Psi + 2\delta\omega^2}{(\Psi^2 + \xi^2)^{1/2}} \right]$$

$$\eta_{\pm} = \frac{[\pm\Psi + (\Psi^2 + \xi^2)^{1/2}]^{1/2}}{2\sqrt{2}\nu_{CPMG}}$$

$$\Psi = k_{ex}^2 - \delta\omega^2 \quad \xi = -2\delta\omega(p_a k_{ex} - p_b k_{ex})$$

where $\delta\omega$ is the chemical shift difference between the ground and excited states, k_{ex} ($= k_{forward} + k_{backward}$) is the exchange rate, p_a is the population of the ground state, and p_b is the population of the excited state. Errors for the exchange parameters were obtained from 1000 runs of Monte Carlo analysis. Outliers were identified using Chauvenet's criterion at a significance level of 96% and omitted from further analysis.³³ Mean values and standard deviations of fitted parameters are reported.

2.6.2. Processing and Analysis of Longitudinal Exchange Data. Peak intensities at the various mixing periods were obtained by summing over 3 × 3 ($t_1 \times t_2$) data points as above. Then a least-squares fitting procedure was applied to determine k_{AB} , k_{BA} , R_1^A and R_1^B by fitting the following expressions:

$$M_{BB}(t)/M_{BB}(0) = \frac{1}{\lambda_1 - \lambda_2} [(a_{11} + \lambda_1)e^{\lambda_1 t} - (a_{11} + \lambda_2)e^{\lambda_2 t}]$$

$$M_{AA}(t)/M_{AA}(0) = \frac{1}{\lambda_1 - \lambda_2} [(a_{22} + \lambda_1)e^{\lambda_1 t} - (a_{22} + \lambda_2)e^{\lambda_2 t}] \quad (3)$$

$$M_A(t)/M_A(0) = \frac{1}{\lambda_1 - \lambda_2} [(a_{22} - a_{21} + \lambda_1)e^{\lambda_1 t} - (a_{22} - a_{21} + \lambda_2)e^{\lambda_2 t}]$$

$$M_B(t)/M_B(0) = \frac{1}{\lambda_1 - \lambda_2} [(a_{11} - a_{12} + \lambda_1)e^{\lambda_1 t} - (a_{11} - a_{12} + \lambda_2)e^{\lambda_2 t}] \quad (4)$$

M_{AA} and M_{BB} are the intensities of the correlation peaks from the ZZ exchange experiment. These intensities are normalized by the peak volumes at zero mixing time ($M_{AA}(0)$ and $M_{BB}(0)$). $M_A(0)/M_B(0)$ and $M_A(t)/M_B(t)$ are the peak intensities of folds A and B at zero mixing time or mixing time t from the T_1 experiment. The eigenvalues of the spin density matrix with magnetization transfer effects from chemical exchange are given by

$$\lambda_{1/2} = \frac{1}{2} [-(a_{11} + a_{22}) \pm [(a_{11} - a_{22})^2 + 4a_{12}a_{21}]^{1/2}]$$

with the elements a_{ij} defined as

$$a_{11} = k_{AB} + R_1^A \quad a_{22} = k_{BA} + R_1^B \quad a_{12} = -k_{BA}$$

$$a_{21} = -k_{AB}$$

The parameters k_{AB} and k_{BA} describe the microscopic rate constants describing the interconversion between the two folding states of RNA 18, while R_1^A and R_1^B are the longitudinal relaxation rates in conformations A and B, respectively. Experimental uncertainties were estimated from 1000 Monte Carlo runs in which synthetic data sets were generated from the best fit values of k_{AB} , k_{BA} , R_1^A , and R_1^B by adding random errors based on the signal-to-noise ratio to the best fit curves. For details of the analysis please refer to ref 31.

3. RESULTS AND DISCUSSION

3.1. Choice of ^{13}C Modification. Our goal was the development of a native, site-specific ^{13}C isotope labeling protocol for the investigation of RNA dynamics by solution NMR spectroscopy. We opted for ($6\text{-}^{13}\text{C}$)pyrimidine as an appropriate modification (Figure 1a).³⁴ The main advantage of

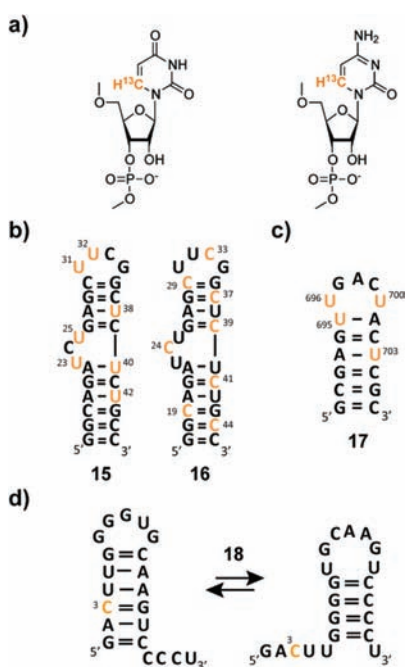


Figure 1. (a) ($6\text{-}^{13}\text{C}$)Uridine (left) and ($6\text{-}^{13}\text{C}$)cytidine (right) modification. (b) HIV-1 TAR RNAs 15 and 16.³⁵ (c) Varkud satellite (VS) stem loop V RNA 17.²⁷ (d) Bistable terminator antiterminator RNA element 18 from the preQ1 riboswitch class I system.²⁶ ^{13}C -labeled residues are highlighted in orange.

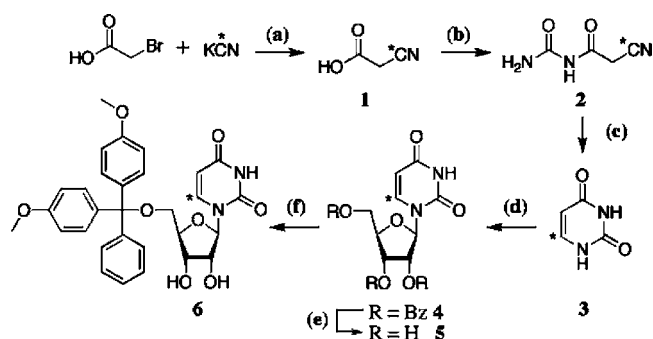
this labeling protocol is that it represents an isolated $^1\text{H}\text{-}^{13}\text{C}$ spin system, for which relaxation dispersion experiments can be conducted in a straightforward manner. Technical issues, normally encountered when relaxation dispersion methods are applied to uniformly $^{13}\text{C}/^{15}\text{N}$ -labeled RNA, e.g., $^{13}\text{C}\text{-}^{13}\text{C}/^{15}\text{N}$ scalar couplings or dipolar couplings and other complex relaxation pathways, are not present in the tailor-made RNAs presented here (Figure 1b–d). Thus, we were able to conduct NMR experiments for studying dynamics in the micro- to millisecond time regime (and beyond) to give interesting insights into functionally important dynamics of RNA.

3.2. Synthesis of $6\text{-}^{13}\text{C}$ -Modified Uridine and Cytidine Phosphoramidites 8, 10, and 14. The key compound in the presented synthesis is the ($6\text{-}^{13}\text{C}$)uracil precursor, which was coupled to an appropriate sugar building block to give the uridine nucleoside, the starting point for all subsequent transformations.

We started our synthesis from ^{13}C -modified potassium cyanide, which was converted into ($3\text{-}^{13}\text{C}$)cyanoacetic acid

(1) via a Kolbe nitrile synthesis using 2-bromoacetic acid.³⁶ Then [($3\text{-}^{13}\text{C}$)cyanoacetyl]urea (2) was obtained by treating compound 1 with urea in the presence of acetic anhydride. In the following step, key compound ($6\text{-}^{13}\text{C}$)uracil (3) was obtained by a reduction of the nitrile and a subsequent ring closure reaction. The reduction was achieved by the use of a palladium catalyst (5% palladium on barium sulfate) under a hydrogen atmosphere. 3 was then coupled to the commercially available ATBR under Vorbrüggen conditions to give the benzoyl-protected uridine nucleoside 4.³⁷ Removal of the benzoyl residues to give ($6\text{-}^{13}\text{C}$)uridine (5) and subsequent tritylation gave $5'\text{-O-DMT-(6-}^{13}\text{C})$ uridine (6) (Scheme 1).

Scheme 1. Synthesis of Intermediate $5'\text{-O-DMT-(6-}^{13}\text{C})$ uridine^a

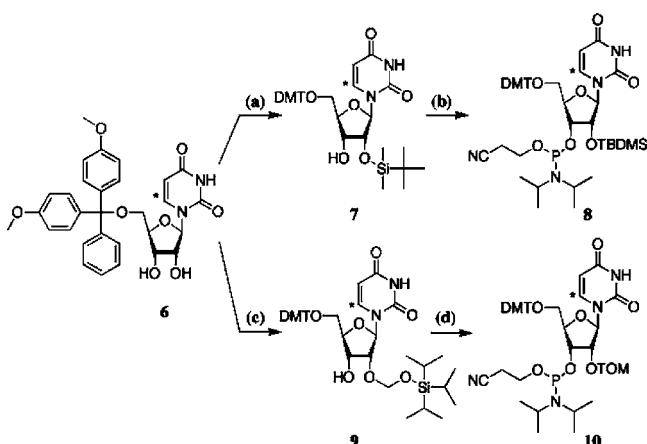


^aReagents and conditions: (a) sodium carbonate, pH 9, 3 h at 80 °C, 20 h at rt, 92%; (b) urea in acetic anhydride, 30 min at 90 °C, 90%; (c) 5% Pd/BaSO₄ in 50% aqueous acetic acid, 36 h at rt, 82%; (d) ATBR, BSA, (TMS)OTf in acetonitrile, 1 h at 60 °C, 98%; (e) CH₃NH₂ in ethanol, 16 h at rt, 90% (related to ($6\text{-}^{13}\text{C}$)uracil used in step d); (f) (DMT)Cl in pyridine, 4 h at rt, 67%. An asterisk indicates ^{13}C .

In the next steps two alternative silyl protection groups for the 2'-hydroxyl group were used. The TBDMS protection group was introduced first, whereas the [(triisopropylsilyl)oxy]methyl group was established by Pitsch et al. more recently.³⁸ The latter is reported to be slightly superior in RNA solid-phase synthesis as the lower steric demand gives higher coupling yields, routinely higher than 98%. In our hands, however, both the TOM- and the TBDMS-($6\text{-}^{13}\text{C}$)uridine building blocks gave similar yields in the respective coupling step by prolonging the coupling time for the TBDMS building block. The TBDMS group was attached at the 2'-hydroxyl group by treating compound 6 with *tert*-butyldimethylsilyl chloride, silver nitrate, and pyridine in anhydrous tetrahydrofuran.³⁹ Finally, the phosphoramidite building block 8 was obtained by treatment with 2'-cyanoethyl *N,N*-diisopropylchlorophosphoramidite (Scheme 2).

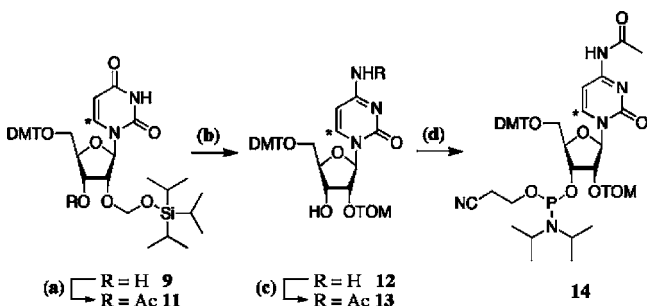
Concurrently, we used the standard protocol published by Pitsch et al. for the synthesis of the 2'-*O*-TOM-protected ($6\text{-}^{13}\text{C}$)uridine building block 10.³⁸ First, 6 was treated with (TOM)Cl in the presence of dibutyltin dichloride and DIPEA to yield both the 2'-*O*-TOM- and 3'-*O*-TOM-protected compounds.⁴⁰ The latter was deprotected with tetrabutylammonium fluoride and again treated with (TOM)Cl. The 2'-*O*-TOM-protected uridine derivative 9 was then transformed under standard conditions to the phosphoramidite building block 10 (Scheme 2).

Starting from $5'\text{-O-DMT-2'-O-TOM-(6-}^{13}\text{C})$ uridine (9), the corresponding cytidine derivative 12 was obtained by a multistep reaction according to published methods.⁴¹ The

Scheme 2. Synthesis of (6-¹³C)Uridine TOM- and TBDMS-Protected Phosphoramidites^a


^aReagents and conditions: (a) (TBDMS)Cl, AgNO₃, pyridine in THF, 4 h at rt, 55%; (b) (CEP)Cl, DIPEA in anhydrous THF, 2 h at rt, 83%; (c) (TOM)Cl, Bu₂SnCl₂, DIPEA in 1,2-dichloroethane, 1.5 h at 80 °C, 30%; (d) (CEP)Cl, DMEA in anhydrous methylene chloride, 2 h at rt, 86%. An asterisk indicates ¹³C.

uridine to cytidine transformation was followed by the acylation of the exocyclic amino functionality, yielding compound 13. Finally, the (6-¹³C)cytidine phosphoramidite 14 was obtained using the phosphitylation reaction conditions as above (Scheme 3). NMR spectra of the phosphoramidite building blocks are included in the Supporting Information (Supporting Figure 1).

Scheme 3. Synthesis of (6-¹³C)Cytidine TOM-Protected Phosphoramidite^a


^aReagents and conditions: (a) Ac₂O, DMAP in pyridine, 5 min at 0 °C, 2 h at rt, 82%; (b) NEt₃, DMAP, (TPS)Cl in methylene chloride, 4 h at rt, then 28% aqueous NH₃ in THF, 18 h at rt, then CH₃NH₂ in ethanol, 45 min at rt, 68%; (c) Ac₂O in anhydrous DMF, 22 h at rt, 89%; (d) (CEP)Cl, DMEA in anhydrous methylene chloride, 2 h at rt, 91%. An asterisk indicates ¹³C.

3.3. Chemical Synthesis of RNA Sequences 15, 16, 17, and 18 Bearing 6-¹³C-Modified Nucleotides. The oligoribonucleotides 15, 16, 17, and 18 comprising up to 27 nucleotides were synthesized using RNA solid-phase synthesis (Figure 1b–d).^{7,26,27,35,42,43} Both the 2'-O-TOM/TBMDs-(6-¹³C)uridine and the 2'-O-TOM-(6-¹³C)cytidine building blocks proved to be suitable for the strand assembly procedure in combination with unlabeled 2'-O-TOM-protected nucleoside phosphoramidites yielding tailor-made site-specifically ¹³C-labeled RNAs. Noteworthy, for the solid-phase synthesis cycle using the 2'-O-TBDMS-(6-¹³C)uridine building block, a prolonged coupling time (4 min vs 2 min, TBDMS vs TOM)

was used to guarantee coupling yields greater than 98% as in the case of the 2'-O-TOM-(6-¹³C)uridine and -cytidine phosphoramidites. After successful assembly of the target RNA, standard deprotection conditions using methylamine in ethanol/water followed by treatment with 1 M tetrabutylammonium fluoride in tetrahydrofuran were used. After purification by anion-exchange HPLC, the homogeneity and the ¹³C isotope enrichment were confirmed for all RNAs by LC-ESI mass spectrometry (Table 1; Supporting Figure 2,

Table 1. Sequence Information and Analytical Data for the ¹³C-Modified RNA Sequences 15, 16, 17, and 18

ID ^a	no. of ¹³ C labels ^b	length ^c	yield ^d /nmol	molecular weight	
				calcd	found
15	7 (U)	27	355	8584.1	8584.4
16	8 (C)	27	510	8585.1	8585.6
17	4 (U)	17	750	5406.3	5406.8
18	1 (C)	21	745	6705.1	6705.1

^aSequence identifier. ^bNucleotide type C = (6-¹³C)cytidine and U = (6-¹³C)uridine. ^cNumber of nucleotides. ^dYield on a 2 μmol synthesis scale.

Supporting Information). We successfully incorporated up to eight ¹³C-modified pyrimidine labels into the target RNA on a synthesis scale of 2 μmol. All syntheses yielded sufficient amounts of oligoribonucleotides for the NMR experiments carried out later (on average 500 nmol, i.e., 1 mM, of sample in 500 μL of volume). This makes our approach competitive with enzymatic methods for which similar yields are obtained.¹⁶

At this point we stress some advantages compared to the standard enzymatic method using T7 RNA polymerase.^{44,45} The solid-phase synthesis of RNA does not have any demands on the sequence composition, especially at the 5'-terminus. Furthermore, labeled and unlabeled phosphoramidites of the same nucleotide type can be used to give site-specifically ¹³C-labeled RNAs on the nucleotide level. Thereby, the problem of resonance overlap can be eliminated or at least reduced. This can be of special interest in the dynamic characterization of a nucleic acid as resonance overlap virtually impedes the data analysis. The approach can in the future also be used to introduce resonance assignment starting points by single 6-¹³C-modified pyrimidine substitutions into the target RNA. In combination with enzymatic isotope labeling, the resonance assignment process for larger RNAs, such as naturally occurring riboswitch aptamer domains comprising up to 50 nucleotides (nt), will be simplified by this method. Currently, the upper limit of the presented approach is set by RNAs comprising more than 55 nucleotides; e.g., for a 52 nt riboswitch aptamer domain, we reproducibly obtain about 100 nmol from a synthesis on a 1.4 μmol scale (unpublished data). Combining two such synthetic runs yields 0.8 mM samples in restricted volume NMR tubes, a concentration range where biomolecular NMR methods to study structure and dynamics can be applied on a high-field spectrometer ideally equipped with cryogenic probe technology.

3.4. ¹³C CPMG Relaxation Dispersion Experiments To Probe Micro- to Millisecond Dynamics. **3.4.1. HIV-1 TAR RNA.** We used CPMG relaxation dispersion experiments to probe pyrimidine nucleobase dynamics of the TAR from HIV-1 in the millisecond time regime. The HIV-1 TAR RNA is a well-known paradigm that nucleic acids can adaptively change their conformation and bind diverse ligands.^{7,46} It was recently

shown that the 27 nt RNA construct (15 and 16) utilizes a conformational selection mechanism to interact with its binding partners, such as argininamide.⁷ These data suggest that the free HIV-1 TAR RNA cycles through multiple conformations resembling ligand-bound states with lifetimes of nano- to picoseconds. For this RNA, we replaced all pyrimidine nucleotides with the corresponding $6\text{-}^{13}\text{C}$ counterpart as discussed in the previous section, resulting in constructs 15 and 16. Via $^1\text{H}\text{-}^{13}\text{C}$ HSQC spectra, the expected labeling pattern was confirmed (Figure 2). With these tailor-made

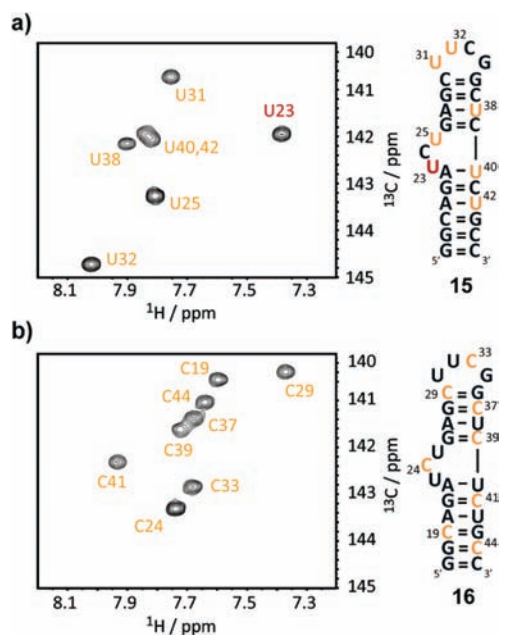


Figure 2. (a) $^1\text{H}\text{-}^{13}\text{C}$ HSQC spectra of the ($6\text{-}^{13}\text{C}$)uridine-labeled HIV-1 TAR RNA 15 and (b) the ($6\text{-}^{13}\text{C}$)cytidine-labeled HIV-1 TAR RNA 16. Assignments were reported previously.⁷ Conditions: 0.7 (15) and 1 (16) mM RNA, 15 mM sodium phosphate, pH 6.4, 25 mM sodium chloride, $\text{H}_2\text{O}/\text{D}_2\text{O} = 9/1$, 25 $^\circ\text{C}$.

RNAs, we were able to probe the HIV-1 TAR system for functional dynamics at micro- to milliseconds using ^{13}C CPMG relaxation dispersion experiments.

Briefly, we could identify only one residue with a nonflat relaxation dispersion profile, namely, uridine 23 (U23; Figure 3a). All the other pyrimidine nucleobases did show flat dispersion profiles in the CPMG RD experiments at 125 and/or 200 MHz carbon Larmor frequency (Figure 3a; Supporting Figure 3, Supporting Information). For the residue U23, data were acquired at two magnetic field strengths (11.7 and 18.8 T), and fitting the data to a two-site exchange process in the intermediate NMR chemical shift time scale according to eq 2 resulted in an excited-state population of $1.0\% \pm 0.6\%$, an exchange rate k_{ex} ($= k_{\text{forward}} + k_{\text{backward}}$) of $2200 \pm 1510 \text{ s}^{-1}$, and a chemical shift difference $\Delta\delta_{\text{RD}}$ between the ground and excited states of $2.4 \pm 0.7 \text{ ppm}$.

This two-state equilibrium fits qualitatively to the previously proposed conformational selection mechanism as U23 undergoes a rigorous structural rearrangement on the addition of the ligand argininamide. In detail, a base triple, U38–A27–U23, is formed on the addition of the ligand, resulting in a drastic chemical shift change for the $6\text{-}^{13}\text{C}$ atom of U23 ($\Delta\delta_{\text{free-ARG}} = 3.3 \text{ ppm}$; Supporting Figure 4, Supporting Information).^{35,42} The carbon shift difference induced by the binding partner is in

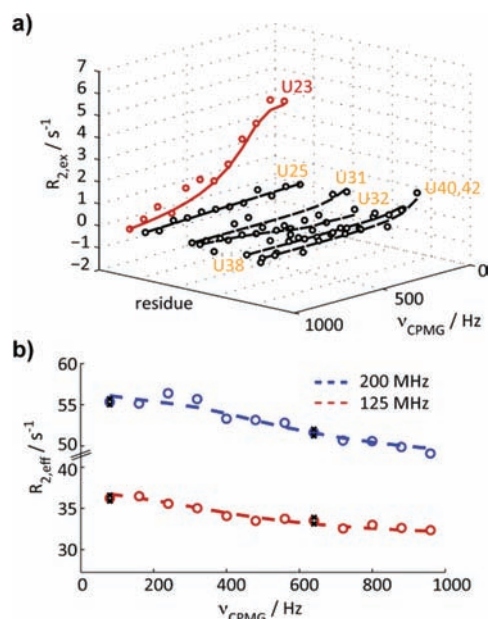


Figure 3. (a) ^{13}C CPMG relaxation dispersion profiles of HIV-1 TAR RNA 15 at 125 MHz carbon Larmor frequency. Dots represent experimental data. Residue U23 shows a nonflat dispersion profile. $R_{2,\text{eff}}$ values at $\nu_{\text{CPMG}} = 960 \text{ Hz}$ were subtracted from the data for display purposes. (b) CPMG dispersion profiles of U23 at 125 (red) and 200 (blue) MHz carbon Larmor frequency, which were used for a quantitative description of the excited state. Dots represent the experimental data. Black times signs represent repeat experiments. The dashed blue and red lines represent the best fits for a two-state equilibrium according to eq 2 in the intermediate exchange regime.

reasonably good agreement with the relaxation dispersion data for U23 ($\Delta\delta_{\text{free-ARG}} = 3.3 \text{ ppm}$ and $\Delta\delta_{\text{RD}} = 2.4 \pm 0.7 \text{ ppm}$). This could point toward a transient formation of the base triple among U38, A27, and U23 found in the excited state. We also conducted CPMG relaxation dispersion experiments for the free HIV-1 TAR RNA 15 at lower (17 $^\circ\text{C}$) and elevated (33 $^\circ\text{C}$) temperatures. In both cases the exchange process for residue U23 was quenched, resulting in flat dispersion profiles (Supporting Figure 5, Supporting Information). We then repeated the CPMG RD NMR experiments in the presence of the ligand argininamide (1/2 and 1 equiv with respect to the RNA). With a reported dissociation constant for the HIV-1 TAR RNA–argininamide complex of approximately 1 mM, the CPMG RD technique is expected to be the appropriate experiment to measure the dynamics (k_{on} and k_{off} rates) of the ligand binding process. Flat relaxation dispersion profiles for the majority of the peaks were observed, indicating that the exchange process either occurs on a time scale not detectable with the CPMG RD experiment or does not involve sufficiently large chemical shift differences (Supporting Figure 6, Supporting Information). Residue U23, however, did show a scattered (and potentially nonflat) relaxation dispersion profile in the presence of argininamide, along with higher than average effective transverse relaxation rates, most due to line broadening arising from the chemical exchange process between the free and the ligand-bound conformations. However, the reduced signal-to-noise ratio of U23 and the concomitant scattering of the experimental data especially at low ν_{CPMG} values impeded a quantitative analysis of the U23 CPMG RD data.

3.4.2. Varkud Satellite Stem Loop V Motif. To further demonstrate the applicability of the ($6\text{-}^{13}\text{C}$)pyrimidine labels in relaxation dispersion experiments, we extended our study on the 17 nt Varkud satellite (VS) stem loop V segment 17 (Figure 4a).^{27,47} The solution structure of this RNA was solved

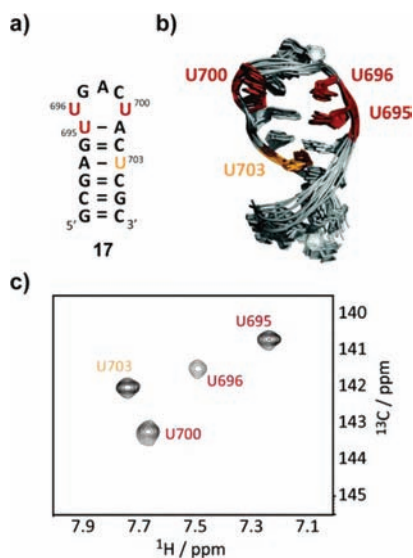


Figure 4. (a) Secondary structure representation of the VS stem loop V motif 17. Uridine residues are color coded as in (b) and (c). (b) Solution structure bundle of 17 with uridines highlighted in red and orange (PDB ID 1TBK).²⁷ (c) ^1H - ^{13}C HSQC spectrum of the ($6\text{-}^{13}\text{C}$)uridine-labeled VS stem loop V motif 17. Assignments were reported previously.²⁷ Conditions: 1 mM RNA, 10 mM Tris·HCl, pH 6.5, 25 mM sodium chloride, $\text{H}_2\text{O}/\text{D}_2\text{O} = 9/1$, 15 $^\circ\text{C}$.

previously (Figure 4b). The observed ^1H - ^{13}C HSQC spectrum of ($6\text{-}^{13}\text{C}$)uridine-modified sequence 17 is in good accordance with that reported (Figure 4c).²⁷ We conducted relaxation dispersion experiments at various temperatures. At 25 $^\circ\text{C}$ residue U696 exhibited an exchange process, which was too fast to be quantified by the CPMG relaxation dispersion technique. This was manifested by a very strong dependence of the effective transverse relaxation rate ($R_{2,\text{eff}}$) on the CPMG pulse frequency (ν_{CPMG}), virtually impairing a reliable analysis of the exchange data. All other residues showed flat or near-flat (U695) dispersion profiles (Supporting Figure 7, Supporting Information).

We then lowered the temperature to 15 $^\circ\text{C}$ and repeated the RD experiments. The temperature change led to observable nonflat dispersion profiles for the loop-closing residue U695 and the loop residues U696 and U700 (Figure 5a). The data could be fitted to a collective motion of these residues for a two-site exchange in the intermediate exchange regime according to the Carver–Richards equation (eq 2) (Figure 5b). We found a population of the excited state of $3.8\% \pm 0.6\%$, an exchange rate $k_{\text{ex}} (= k_{\text{forward}} + k_{\text{backward}})$ of 3080 ± 840 Hz, and chemical shift differences between the ground and excited states of 0.7 ± 0.4 ppm (U695), 3.1 ± 0.5 ppm (U696), and 1.0 ± 0.2 ppm (U700). Residue U703 did not show any detectable micro- to millisecond dynamics as expected for a nucleotide locked up in a stable Watson–Crick base pair. The observed dynamics in the millisecond time regime of residues U695 and U696 and especially U700 could be crucial for the function of the ribozyme, as the stem loop V motif is involved in a loop–loop interaction with stem loop I, leading to a shifted, active

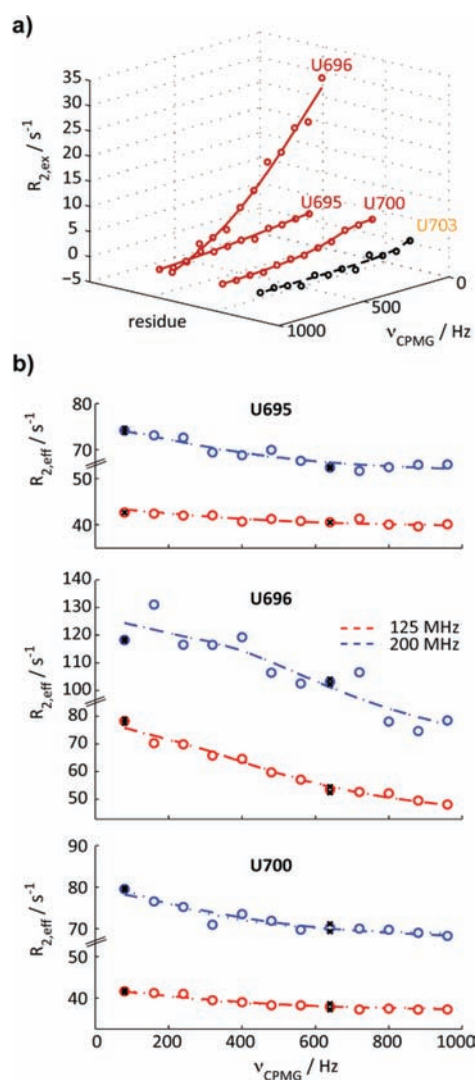


Figure 5. (a) ^{13}C CPMG relaxation dispersion profiles of VS stem loop V motif 17 at 125 MHz carbon Larmor frequency and 15 $^\circ\text{C}$. Dots represent experimental data. Residues U695, U696, and U700 show nonflat dispersion profiles. $R_{2,\text{eff}}$ values at $\nu_{\text{CPMG}} = 960$ Hz were subtracted from the data for display purposes. (b) CPMG dispersion profiles of U695, U696, and U700 at 125 (red) and 200 (blue) MHz carbon Larmor frequency, which were used for a quantitative analysis of the excited state. Dots represent the experimental data. Black times signs represent repeat experiments. The dashed and dotted blue and red lines represent the individual and global fits according to eq 2 for a two-state equilibrium in the intermediate exchange regime.

conformation of the substrate hairpin I.^{27,48} A detailed analysis of the potentially functional dynamics underlying the loop–loop kissing tertiary interaction in the presence of magnesium ions and the stem loop I motif using ($6\text{-}^{13}\text{C}$)uridine and ($6\text{-}^{13}\text{C}$)cytidine labels is currently being carried out in our laboratory and will be reported elsewhere.

3.5. ZZ Exchange Experiments To Probe Secondary Structure Refolding Kinetics. So far we have shown the applicability of ($6\text{-}^{13}\text{C}$)pyrimidine spin-labels as probes of micro- to millisecond nucleic acid dynamics. It was recently shown that slower dynamics with folding times of a few milliseconds to seconds can be of special importance for the biological function of riboswitch RNAs.^{2,49–51} Riboswitches are a class of nucleic acids for which structural flexibility is inherently linked to their biological function. These RNAs

switch their tertiary/secondary structure in response to the presence or absence of a low-molecular-weight metabolite.^{52–54} We and others previously investigated the mode of action of the preQ₁ class I riboswitch system in detail.^{26,55,56} In the previous work a bistable terminator antiterminator sequence, 18, was identified (Figure 6a).²⁶

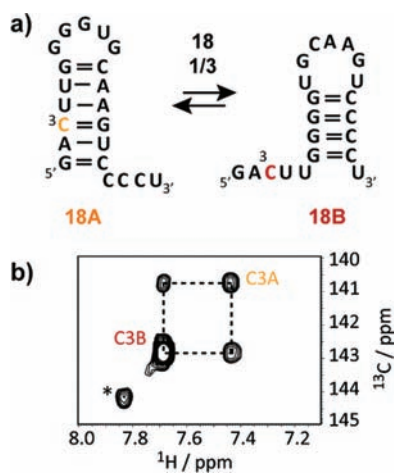


Figure 6. (a) Secondary structure equilibrium of terminator antiterminator RNA 18 with a population of 18A/18B of approximately 35/65. (b) ZZ exchange spectrum of 18 at a mixing time of 200 ms and at 33 °C. The resonance presumably arising from the homoduplex is marked with an asterisk. Conditions: 1 mM RNA, 25 mM sodium arsenate, pH 6.5, D₂O, 33 °C.

We now were interested in the kinetics underlying the two-state secondary structure equilibrium between folds 18A and 18B (Figure 6a). For that purpose, we introduced a single (6-¹³C)cytidine substitution into the RNA and used ¹³C longitudinal exchange NMR spectroscopy to probe the refolding kinetics. Peak integration yielded the equilibrium constant, which was in favor of fold 18B ($K_{AB} = 3$). As expected we found two correlation peaks (C3A and C3B) for C3 in the ¹³C ZZ exchange spectrum of RNA 18 for which exchange peaks could be identified (Figure 6b). Fold assignment was achieved using a truncated reference sequence (Supporting Figure 8, Supporting Information). The forward and backward folding rates of the secondary structure equilibrium were determined at 33 °C using an approach recently introduced by analyzing longitudinal relaxation rates with and without exchange contribution (Figure 7). We found a forward rate constant k_{AB} of $3.3 \pm 0.1 \text{ s}^{-1}$ and a rate constant k_{BA} for the folding process from state B to state A of $1.4 \pm 0.3 \text{ s}^{-1}$, giving a good agreement with the equilibrium constant obtained from peak integration ($K_{AB} = 3$ and $K_{AB} = k_{AB}/k_{BA} = 2.4$). Using our ¹³C labeling method approach, we were thus able to characterize the refolding kinetics of the terminator antiterminator RNA 18 in unperturbed equilibrium under near physiological conditions.

4. CONCLUSIONS

Within this work we established a fully native ¹³C labeling approach for RNA relying on (6-¹³C)pyrimidine amidite building blocks suitable for oligonucleotide solid-phase synthesis. This isolated ¹H–¹³C spin was used to address RNA nucleobase dynamics in the milli- to microsecond time regime by applying the CPMG relaxation dispersion technique. The

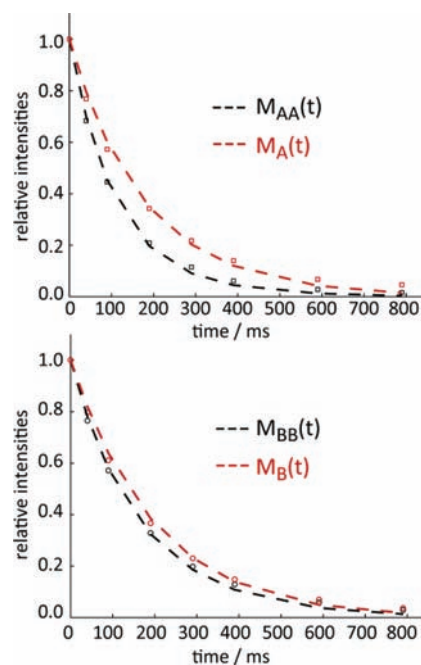


Figure 7. Normalized partial peak volumes of $M_A(t)$ and $M_{AA}(t)$ (red and black rectangles) and $M_B(t)$ and $M_{BB}(t)$ (red and black circles) corresponding to the correlation peaks of spin-label C3 of the ZZ exchange ($M_{AA/BB}(t)$) and T_1 ($M_{A/B}(t)$) experiments, together with best fit curves (dashed red and black lines). All four curves were obtained by simultaneously fitting the experimental data to eqs 3 and 4. Rate constants $k_{AB} = 3.3 \pm 0.1 \text{ s}^{-1}$ and $k_{BA} = 1.4 \pm 0.3 \text{ s}^{-1}$ and longitudinal relaxation rates $R_1^A = 5.78 \pm 0.08 \text{ s}^{-1}$ and $R_1^B = 4.93 \pm 0.13 \text{ s}^{-1}$ for the refolding reaction 18A to 18B and back for residue C3 were obtained.

¹³C-isotope-modified pyrimidines were introduced into two biologically relevant RNAs, the HIV-1 TAR RNAs 15 and 16, and the Varkud satellite stem loop V motif 17. For both nucleic acid fragments, residues exhibiting dynamics on the milli- to microsecond time scale could be identified.

The dynamics of U23 of the HIV-1 TAR RNA could arise from an excited state, where a base triple including U38, A27, and U23 is transiently formed resembling the argininamide-bound state.³⁵ This further corroborates the conformation selection mechanism of the HIV-1 TAR RNA previously proposed by solution and solid-state NMR.^{7,46} Within the 17 nt long Varkud satellite stem loop motif V 17, three residues, U695, U696, and U700, exhibited a nonflat CPMG relaxation dispersion profile. The data could be fit to collective motion of the three residues, which could be important for a loop–loop kissing tertiary interaction.^{47,48}

To further illustrate the fields of application of our (6-¹³C)pyrimidine labeling protocol, the kinetics of a secondary structure refolding reaction was characterized. A bistable terminator antiterminator RNA element (18) of the preQ₁ class I riboswitch was labeled with a single (6-¹³C)cytidine residue, and longitudinal exchange spectroscopy yielded the forward and backward rates of the secondary structure equilibrium.

The (6-¹³C)pyrimidine labels have proven to be generally applicable to study conformational dynamics and the refolding kinetics in RNAs comprising up to 30 nucleotides using standard NMR techniques. Currently, the limit by the presented approach is set by RNAs comprising more than 55

nt as the yield of the solid-phase synthesis methodology drops significantly with the increasing size of the oligonucleotide. For such larger 50 nt RNAs pulse sequences comprising a TROSY element will be particularly useful.^{57,58} Therefore, the ¹³C label can be shifted to position C5, which shows more favorable TROSY properties,⁵⁹ simply by using commercially available (2-¹³C)-2-bromoacetic acid and unlabeled potassium cyanide as starting materials. These 5-¹³C-labeled pyrimidine building blocks could further be deuterated at position C6, resulting in even more advantageous relaxation properties,⁶⁰ a crucial prerequisite for the NMR spectroscopic investigation of large biomolecular complexes. The labeling protocol will in the near future also be expanded to (8-¹³C)purine building blocks and will be used to site-specifically modify functional nucleic acids, such as riboswitch aptamer domains or ribozymes, to give interesting insights into the functional dynamics of these RNAs.^{61,62}

■ ASSOCIATED CONTENT

■ Supporting Information

NMR spectra of phosphoramidite building blocks **8**, **10**, and **14**, mass spectra of ¹³C-modified RNAs **15**, **16**, **17**, and **18**, CPMG dispersion profiles of (6-¹³C)cytidine-modified HIV-1 TAR RNA **16**, titration of (6-¹³C)uridine-modified HIV-1 TAR RNA **15** with argininamide, CPMG dispersion profiles of (6-¹³C)-uridine-modified HIV-1 TAR RNA **15** at 17 and 33 °C and in the presence of L-argininamide, CPMG dispersion profiles of (6-¹³C)uridine-modified VS stem loop V RNA **17** at 25 °C, fold assignment of RNA **18** using a truncated reference sequence and a H₂O NOESY experiment, and table summarizing the NMR experiments applied to obtain data on the dynamics of RNAs **15**, **16**, **17**, and **18** and the respective results. This material is available free of charge via the Internet at <http://pubs.acs.org>.

■ AUTHOR INFORMATION

Corresponding Author

christoph.kreutz@uibk.ac.at

Notes

The authors declare no competing financial interest.

■ ACKNOWLEDGMENTS

C.K. thanks Ronald Micura (Innsbruck), Bernhard Kraeutler (Innsbruck), and Robert Konrat (Vienna) for continuous support and scientific discussions. We thank Karin Kloiber for setting up some of the relaxation dispersion experiments. This work was supported by the Tyrolean Science Fund TWF (Project 95421 to C.K.), a Young Talents Grant from the University of Innsbruck (to C.K.), and the Austrian Science Fund FWF (Grant I844-N17 to C.K.).

■ REFERENCES

- (1) Palmer, A. G.; Kroenke, C. D.; Loria, J. P. *Methods Enzymol.* **2001**, *339*, 204.
- (2) Al-Hashimi, H. M.; Walter, N. G. *Curr. Opin. Struct. Biol.* **2008**, *18*, 321.
- (3) Latham, M. P.; Brown, D. J.; McCallum, S. A.; Pardi, A. *ChemBioChem* **2005**, *6*, 1492.
- (4) Mittermaier, A. K.; Kay, L. E. *Trends Biochem. Sci.* **2009**, *34*, 601.
- (5) Akke, M.; Fiala, R.; Jiang, F.; Patel, D.; Palmer, A. G. *RNA* **1997**, *3*, 702.
- (6) Getz, M.; Sun, X.; Casiano-Negroni, A.; Zhang, Q.; Al-Hashimi, H. M. *Biopolymers* **2007**, *86*, 384.
- (7) Zhang, Q.; Sun, X.; Watt, E. D.; Al-Hashimi, H. M. *Science* **2006**, *311*, 653.
- (8) Lipari, G.; Szabo, A. J. *Am. Chem. Soc.* **1982**, *104*, 4546.
- (9) Lipari, G.; Szabo, A. J. *Am. Chem. Soc.* **1982**, *104*, 4559.
- (10) Korzhnev, D. M.; Religa, T. L.; Banachewicz, W.; Fersht, A. R.; Kay, L. E. *Science* **2010**, *329*, 1312.
- (11) Shajani, Z.; Varani, G. *Biopolymers* **2007**, *86*, 348.
- (12) Quant, S.; Wechselberger, R. W.; Wolter, M. A.; Woerner, K. H.; Schell, P.; Engels, J. W.; Griesinger, C.; Schwalbe, H. *Tetrahedron Lett.* **1994**, *35*, 6649.
- (13) Batey, R. T.; Cloutier, N.; Mao, H.; Williamson, J. R. *Nucleic Acids Res.* **1996**, *24*, 4836.
- (14) Batey, R. T.; Inada, M.; Kujawinski, E.; Puglisi, J. D.; Williamson, J. R. *Nucleic Acids Res.* **1992**, *20*, 4515.
- (15) Nikonowicz, E. P.; Pardi, A. *J. Mol. Biol.* **1993**, *232*, 1141.
- (16) Lu, K.; Miyazaki, Y.; Summers, M. J. *Biomol. NMR* **2010**, *46*, 113.
- (17) Thakur, C.; Sama, J.; Jackson, M.; Chen, B.; Dayie, T. J. *Biomol. NMR* **2010**, *48*, 179.
- (18) Johnson, J. E.; Julien, K. R.; Hoogstraten, C. G. J. *Biomol. NMR* **2006**, *35*, 261.
- (19) Thakur, C.; Sama, J.; Jackson, M.; Chen, B.; Dayie, T. J. *Biomol. NMR* **2010**, *48*, 179.
- (20) Schultheisz, H. L.; Szymczyna, B. R.; Scott, L. G.; Williamson, J. R. *ACS Chem. Biol.* **2008**, *3*, 499.
- (21) Schultheisz, H. L.; Szymczyna, B. R.; Scott, L. G.; Williamson, J. R. *J. Am. Chem. Soc.* **2010**, *133*, 297.
- (22) Johnson, J. E.; Hoogstraten, C. G. J. *Am. Chem. Soc.* **2008**, *130*, 16757.
- (23) Nikolova, E. N.; Gottardo, F. L.; Al-Hashimi, H. M. *J. Am. Chem. Soc.* **2012**, *134*, 3667.
- (24) Kloiber, K.; Spitzer, R.; Tollinger, M.; Konrat, R.; Kreutz, C. *Nucleic Acids Res.* **2011**, *39*, 4340.
- (25) Micura, R. *Angew. Chem., Int. Ed.* **2002**, *41*, 2265.
- (26) Rieder, U.; Kreutz, C.; Micura, R. *Proc. Natl. Acad. Sci. U.S.A.* **2010**, *107*, 10804.
- (27) Campbell, D. O.; Legault, P. *Biochemistry* **2005**, *44*, 4157.
- (28) Hwang, T. L.; Shaka, A. J. *J. Magn. Reson., Ser. A* **1995**, *112*, 275.
- (29) Delaglio, F.; Grzesiek, S.; Vuister, G. W.; Zhu, G.; Pfeifer, J.; Bax, A. J. *Biomol. NMR* **1995**, *6*, 277.
- (30) Tollinger, M.; Skrynnikov, N. R.; Mulder, F. A.; Forman-Kay, J. D.; Kay, L. E. *J. Am. Chem. Soc.* **2001**, *123*, 11341.
- (31) Kloiber, K.; Spitzer, R.; Grutsch, S.; Kreutz, C.; Tollinger, M. *J. Biomol. NMR* **2011**, *51*, 123.
- (32) Carver, J. P.; Richards, R. E. *J. Magn. Reson. (1969–1992)* **1972**, *6*, 89.
- (33) Taylor, J. R. *An Introduction to Error Analysis: The Study of Uncertainties in Physical Measurements*, 2nd ed.; University Science Books: Sausalito, CA, 1997.
- (34) SantaLucia, J.; Shen, L. X.; Cai, Z.; Lewis, H.; Tinoco, I. *Nucleic Acids Res.* **1995**, *23*, 4913.
- (35) Puglisi, J. D.; Tan, R.; Calnan, B. J.; Frankel, A. D.; Williamson. *Science* **1992**, *257*, 76.
- (36) Triplett, J. W.; Mack, S. W.; Smith, S. L.; Digenis, G. A. *J. Labelled Compd. Radiopharm.* **1978**, *14*, 35.
- (37) Vorbrüggen, H.; Krolkiewicz, K.; Bennua, B. *Chem. Ber.* **1981**, *114*, 1234.
- (38) Pitsch, S.; Weiss, P. A. *Current Protocols in Nucleic Acid Chemistry*; John Wiley & Sons, Inc.: New York, 2001.
- (39) Milecki, J.; Zamaratski, E.; Maltseva, T. V.; Foldesi, A.; Adamiak, R. W.; Chattopadhyaya, J. *Tetrahedron* **1999**, *55*, 6603.
- (40) Wenter, P.; Reymond, L.; Auweter, S. D.; Allain, F. H. T.; Pitsch, S. *Nucleic Acids Res.* **2006**, *34*, e79.
- (41) Hoebartner, C.; Micura, R. *J. Am. Chem. Soc.* **2004**, *126*, 1141.
- (42) Pitt, S. W.; Majumdar, A.; Serganov, A.; Patel, D. J.; Al-Hashimi, H. M. *J. Mol. Biol.* **2004**, *338*, 7.
- (43) Aboul-ela, F.; Karn, J.; Varani, G. *Nucleic Acids Res.* **1996**, *24*, 3974.

- (44) Milligan, J. F.; Groebe, D. R.; Witherell, G. W.; Uhlenbeck, O. C. *Nucleic Acids Res.* **1987**, *15*, 8783.
- (45) Milligan, J. F.; Uhlenbeck, O. C. *Methods Enzymol.* **1989**, *180*, 51.
- (46) Olsen, G. L.; Bardaro, M. F.; Echodu, D. C.; Drobny, G. P.; Varani, G. J. *Am. Chem. Soc.* **2009**, *132*, 303.
- (47) Campbell, D. O.; Bouchard, P.; Desjardins, G.; Legault, P. *Biochemistry* **2006**, *45*, 10591.
- (48) Bouchard, P.; Lacroix-Labonte, J.; Desjardins, G.; Lampron, P.; Lisi, V.; Lemieux, S.; Major, F.; Legault, P. *RNA* **2008**, *14*, 736.
- (49) Schwalbe, H.; Buck, J.; Fürtig, B.; Noeske, J.; Wöhnert, J. *Angew. Chem., Int. Ed.* **2007**, *46*, 1212.
- (50) Rinnenthal, J.; Buck, J.; Ferner, J.; Wacker, A.; Fürtig, B.; Schwalbe, H. *Acc. Chem. Res.* **2011**, *44*, 1292.
- (51) Al-Hashimi, H. M. *Biopolymers* **2007**, *86*, 345.
- (52) Coppins, R. L.; Hall, K. B.; Groisman, E. A. *Curr. Opin. Microbiol.* **2007**, *10*, 176.
- (53) Serganov, A. *Curr. Opin. Struct. Biol.* **2009**, *19*, 251.
- (54) Tucker, B. J.; Breaker, R. R. *Curr. Opin. Struct. Biol.* **2005**, *15*, 342.
- (55) Rieder, U.; Lang, K.; Kreutz, C.; Polacek, N.; Micura, R. *ChemBioChem* **2009**, *10*, 1141.
- (56) Kang, M.; Peterson, R.; Feigon, J. *Mol. Cell* **2009**, *33*, 784.
- (57) Brutscher, B.; Boisbouvier, J.; Pardi, A.; Marion, D.; Simorre, J.-P. *J. Am. Chem. Soc.* **1998**, *120*, 11845.
- (58) Fiala, R.; Czernek, J.; Sklenář, V. *J. Biomol. NMR* **2000**, *16*, 291.
- (59) Boisbouvier, J.; Bryce, D.; O'Neil-Cabello, E.; Nikonowicz, E.; Bax, A. J. *Biomol. NMR* **2004**, *30*, 287.
- (60) Huang, X.; Yu, P.; LeProust, E.; Gao, X. *Nucleic Acids Res.* **1997**, *25*, 4758.
- (61) Edwards, T. E.; Klein, D. J.; Ferré D'Amaré, A. R. *Curr. Opin. Struct. Biol.* **2007**, *17*, 273.
- (62) Fürtig, B.; Buck, J.; Richter, C.; Schwalbe, H. In *Methods in Molecular Biology*; Hartig, J. S., Ed.; Humana Press: Totowa, NJ, 2012; Vol. 848, p 185.